THE JOURNAL OF BIOLOGICAL CHEMISTRY VOL. 285, NO. 23, pp. 17301–17309, June 4, 2010

Survival Signals of Hepatic Stellate Cells in Liver Regeneration Are Regulated by Glycosylation Changes in Rat Vitronectin, Especially Decreased Sialylation*[S]

Received for publication, October 19, 2009, and in revised form, March 23, 2010 Published, JBC Papers in Press, March 24, 2010, DOI 10.1074/jbc.M109.077016

Kotone Sano[‡], Yasunori Miyamoto[‡], Nana Kawasaki[§], Noritaka Hashii[§], Satsuki Itoh[§], Misaki Murase[‡], Kimie Date[‡], Miki Yokoyama[¶], Chihiro Sato[‖], Ken Kitajima[‖], and Haruko Ogawa[‡1]

From the [‡]Graduate School of Humanities and Sciences and The Glycoscience Institute, Ochanomizu University, Tokyo 112-8610, Ochanomizu, the [§]Division of Biological Chemistry and Biologicals, National Institute of Health Sciences, Tokyo 158-8501, the [¶]Department of Hard Tissue Engineering, Graduate School, Tokyo Medical and Dental University, Tokyo 113-8510, and the [‖]Bioscience and Biotechnology Center, Nagoya University, Nagoya 464-8610, Japan

The extracellular matrix (ECM) molecules play important roles in many biological and pathological processes. During tissue remodeling, the ECM molecules that are glycosylated are different from those of normal tissue owing to changes in the expression of many proteins that are responsible for glycan synthesis. Vitronectin (VN) is a major ECM molecule that recognizes integrin on hepatic stellate cells (HSCs). The present study attempted to elucidate how changes in VN glycans modulate the survival of HSCs, which play a critical role in liver regeneration. Plasma VN was purified from partially hepatectomized (PH) and sham-operated (SH) rats at 24 h after operation and non-operated (NO) rats. Adhesion of rat HSCs (rHSCs), together with phosphorylation of focal adhesion kinase, in PH-VN was decreased to one-half of that in NO- or SH-VN. Spreading of rHSCs on desialylated NO-VN was decreased to one-half of that of control VN, indicating the importance of sialylation of VN for activation of HSCs. Liquid chromatography/multiple-stage mass spectrometry analysis of Glu-C glycopeptides of each VN determined the site-specific glycosylation. In addition to the major biantennary complex-type *N*-glycans, hybrid-type *N*-glycans were site-specifically present at Asn^{167}. Highly sialylated *O*-glycans were found to be present in the Thr^{110}–Thr^{124} region. In PH-VN, the disialyl *O*-glycans and complex-type *N*-glycans were decreased while core-fucosylated *N*-glycans were increased. In addition, immunodetection after two-dimensional PAGE indicated the presence of hyper- and hyposialylated molecules in each VN and showed that hypersialylation was markedly attenuated in PH-VN. This study proposes that the alteration of VN glycosylation modulates the substrate adhesion to rat HSCs, which is responsible for matrix restructuring.

The extracellular matrix (ECM)[2] surrounding cells plays an important role in many biological and pathological processes, including inflammation, tissue remodeling, and invasion by cancer cells (1). ECM is composed of many kinds of adhesive glycoproteins that regulate cellular signaling, motility, and proliferation (1). During tissue remodeling, the glycoconjugates synthesized by cells are different from those of normal tissues owing to the changes in the expression of many proteins that are responsible for glycan synthesis, such as glycosyl transferases, glycosidases, and transporters (2). There is increasing evidence that glycosylation post-translationally modulates biological phenomena by altering the activity and specificity or controlling the stability of various glycoproteins through biosignaling functions of oligosaccharides (2).

Vitronectin (VN) is a multifunctional glycoprotein that originates mainly in hepatocytes and circulates in the blood stream at high concentrations (0.2 mg/ml in humans) (3). Most VN in normal plasma is in an inactive monomer form that does not bind to various ligands. VN acquires these binding activities *in vitro* on treatment with urea or heating through a conformational transition of the native inactive form to an active form. Corresponding activation is considered to occur *in vivo* in the presence of heparin or through the formation of VN complexes such as VN-thrombin-AT-III, VN-terminal complement proteins, and VN-type-I plasmingen activator inhibitor, whereas VN is considered to exist in active multimeric tissue forms when deposited in the ECM.

VN plays a crucial role in regulating the humoral immune system and blood coagulation through binding to complements and interaction with heparin and anti-thrombin III complexes, respectively (4, 5). VN is also present as an ECM component in the liver, as well as various other organs, including skeletal muscle, kidney, and brain (6, 7). VN regulates pericellular proteolysis during tissue remodeling and fibrinolysis through binding

* This work was supported in part by Japan Society for the Promotion of Science Grant 12995 (to K. S.), a fellowship of the Hayashi Memorial Foundation for Female Natural Scientists (to K. S.), and Grants-in-aid for Scientific Research on Priority Areas 15040209 and 17046004 (to H. O.) from the Ministry of Education, Culture, Sports, Science, and Technology.

[S] The on-line version of this article (available at http://www.jbc.org) contains supplemental Fig. 1.

[1] To whom correspondence should be addressed: Graduate School of Humanities and Sciences, Ochanomizu University, 2-1-1 Otsuka, Bunkyo-ku, Tokyo, 112-8610 Japan. Tel.: 03-5978-5343; Fax: 03-5978-5343; E-mail: ogawa.haruko@ocha.ac.jp.

[2] The abbreviations used are: ECM, extracellular matrix; FAK, focal adhesion kinase; HRP, horseradish peroxidase; HSC, hepatic stellate cell; NO, non-operated; PH, partially hepatectomized; PNGase F, peptide-*N*4-(*N*-acetyl-β-D-glucosaminyl)asparagine amidase from *F. meningosepticum*; rHSC, rat hepatic stellate cell; SH, sham-operated; VN, vitronectin; PA, pyridylaminated; LC, liquid chromatography; ESI, electrospray ionization; MS, mass spectrometry; MS^n, multiple-stage mass spectrometry; MS^2, two-stage mass spectrometry; MS^3, three-stage mass spectrometry; MS^4, four-stage mass spectrometry.

with type-1 plasminogen activator inhibitor, urokinase-type plasminogen activator, and urokinase receptor (3, 7–9). Besides this function, VN plays a key role in cell adhesion and cellular motility during tissue remodeling through binding to major ECM receptors, integrins such as $\alpha v\beta 1$, $\alpha v\beta 3$, $\alpha v\beta 5$, $\alpha v\beta 6$, and $\alpha v\beta 8$, and other ECM components like collagen and proteoglycans (3). Therefore, VN simultaneously modulates cell behavior and pericellular proteolysis in the ECM during tissue-remodeling processes.

The liver has a strong capacity to regenerate, and partial hepatectomy is often used to study liver regeneration mechanisms, but many aspects of this complex mechanism are unknown, especially the regulation of each ECM glycoprotein activity by glycosylation. In our preceding study, we showed that both the *N*-glycosylation sites (10) and the *N*-glycan structures are well conserved among mammalian VNs (11–13), and several important ligand-binding activities of VN were found to be significantly affected by changes in VN *N*-glycosylation *in vitro* (14).

Further study demonstrated that multimerization of rat VN increases during liver regeneration after partial hepatectomy and that increases in the collagen-binding activity are synchronized with the glycan changes *in vivo* (15). The molecular mass of VN purified from partially hepatectomized (PH-VN) rats at 24 h had shrunk to 65 kDa compared with the 68–69 kDa of VNs from sham-operated (SH) and non-operated (NO) rats. The reduction of molecular mass was due to a decrease in the carbohydrate concentration of PH-VN, which was two-thirds that of SH-VN and one-third that of NO-VN (15). Because increased multimerization and enhanced collagen binding were induced by enzymatic desialylation of VN, the marked increase in collagen-binding activity was attributable to the increased multimerization induced by glycosylation alterations during liver regeneration after partial hepatectomy of rats (16, 17). We subsequently determined the details of the glycan structures of fibronectin synthesized in the early stage of liver regeneration (18).

The present study attempted to determine the structure and changes of rat VN glycans during liver regeneration with a particular focus on the relationship between hepatic stellate cell (HSC) adhesion and the glycosylation of VN. Because HSCs are the major source of the newly synthesized ECM during hepatic fibrosis, survival or apoptosis of HSCs is critical for the development or resolution, respectively, of liver fibrosis in chronic liver diseases (19). The present findings provide novel insight into the significance of VN glycosylation in regulating HSC survival during tissue remodeling.

EXPERIMENTAL PROCEDURES

Materials—Rat VNs were purified from plasma by two-step heparin affinity chromatography before and after urea treatment as described previously (20). Neuraminidase (*Vibrio cholerae*) and recombinant peptide-*N*4-(*N*-acetyl-β-D-glucosaminyl)asparagine amidase from *Flavobacterium meningosepticum* (PNGase F) were purchased from Roche Diagnostics (Mannheim, Germany). Unconjugated rabbit anti-human VN IgGs and horseradish peroxidase (HRP)-conjugated sheep anti-rabbit IgGs were purchased from The Binding Site (Birmingham, UK). Biotinylated *Sambucus nigra* agglutinin was prepared in our laboratory as previously described (21). Monoclonal antibody S2–566 was prepared as described previously (22). rHSCs were provided by Dr. M. Sato (Akita University, Akita, Japan).

Animals—Male Wistar rats aged 5 weeks (weighing ~110 g, Nihon Clea, Tokyo) were maintained at a constant temperature (23.5 °C) for 12 h in light (6:00 am to 6:00 pm) and dark. Two-thirds partial hepatectomy was performed under diethyl ether anesthesia as described previously (23). Sham-operated rats were anesthetized and operated on in the same way as partially hepatectomized rats, except that the liver was not resected. Plasma samples were collected at 24 h after operations and stored at −80 °C until use.

Glycosidase Digestion of VN—Enzymatic deglycosylation of VN was performed as described previously (15). For desialylation, VN (32 μg/200 μl) was dialyzed against 50 mM acetate buffer containing 4 mM $CaCl_2$ (pH 5.5) and treated with neuraminidase (0.001 unit) at 37 °C overnight. For de-*N*-glycosylation, VN (32 μg/200 μl) was dialyzed against 10 mM phosphate buffer (pH 7.5) containing 0.13 M NaCl and 5 mM EDTA and digested with PNGase F (0.2 unit) at 37 °C for 48 h. For controls, the procedures were performed without the enzymes. The treated VNs were dialyzed against Tris-buffered saline (10 mM Tris-HCl (pH 7.5) containing 0.14 M NaCl). Desialylation or de-*N*-glycosylation was ascertained by both the behavior on SDS-PAGE and the loss of reactivity with biotinylated *S. nigra* agglutinin on Western blotting.

Cell Spreading and Focal Adhesion Kinase Phosphorylation Analysis—rHSCs were grown in Dulbecco's modified Eagle's medium supplemented with 10% fetal bovine serum. For cell-spread analysis, wells of 96-well tissue culture plates were precoated with 0–10 μg/ml VNs. We previously demonstrated that the coating efficiency of VN to the well did not differ in the concentration range examined (15). rHSCs (1×10^5 cells) were placed in wells in 100 μl of adhesion medium (150 mM NaCl, 3 mM KCl, 0.5 mM $MgCl_2$, 6 mM Na_2HPO_4, 1 mM KH_2PO_4, and 1 mM $CaCl_2$, pH 7.3). After incubation for various times at 37 °C in 5% CO_2, the cells were fixed in 12% (w/w) formaldehyde for the adhesion assay. Cell-spreading activity was quantified by determining the ratio of the number of spreading cells to the total number of cells in 3 microscope fields/well. For the focal adhesion kinase (FAK) phosphorylation assay, the cells were washed with ice-cold phosphate-buffered saline (10 mM phosphate buffer (pH 7.5) containing 0.13 M NaCl), lysed in lysis buffer (100 mM Tris-HCl, pH 7.5, 1% Triton X-100, 1% EDTA, 10% glycerol, and 1/100 (v/v) phosphatase inhibitor mixture II (Sigma) and Complete Mini EDTA-free protease inhibitor mixture tablets (1 tablet/150 ml), Roche Diagnostics) on ice, and centrifuged at 15,000 rpm for 20 min at 4 °C. The supernatants were collected and subjected to SDS-PAGE, followed by blotting onto polyvinylidene difluoride membrane. The membrane was blocked with 5% skim milk and incubated with HRP-conjugated mouse monoclonal anti-phosphotyrosine IgG, PY20 (Abcam, Cambridge Science Park, UK), anti-FAK IgG, sc-558 (Santa Cruz Biotechnology, Santa Cruz, CA) or anti-β-actin IgG antibodies for 1 h each, and detection was performed by using ECL-Plus according to the manufacturer's instructions.

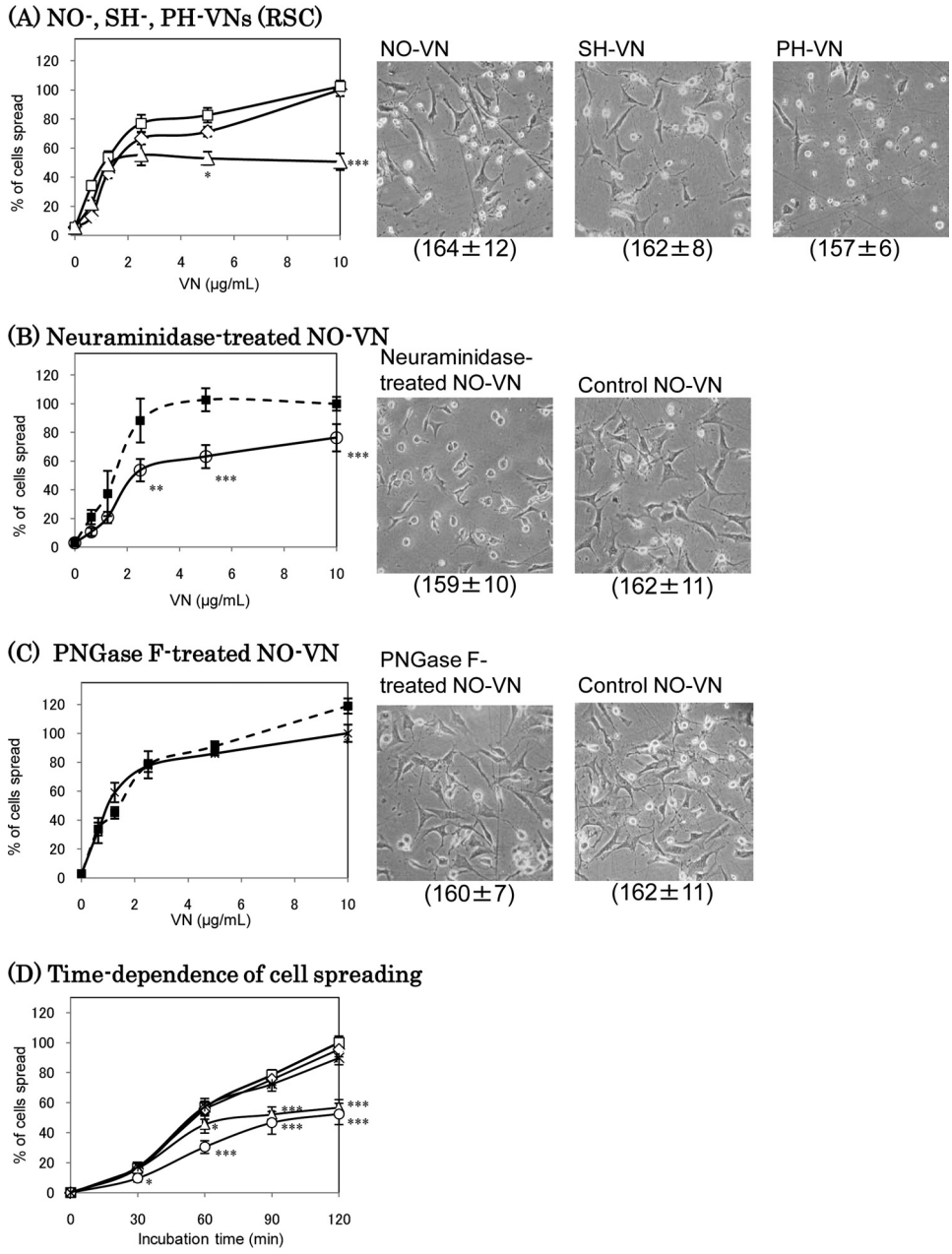

FIGURE 1. **Spreading of rHSCs on VNs.** rHSCs (1×10^5 cells/ml) were plated on substrates coated with various concentrations (*A–C*) of VNs purified from NO (□), SH (◇), or PH (△) rats (*A* and *D*) or desialylated (*B*, ○) or de-*N*-glycosylated (*C*, ∗) VN, or a VN control incubated without enzyme (*B–D*, ■). After 90-min incubation at 37 °C in 5% CO_2, spreading activities of the cells were assessed as described in the text and expressed by taking those on 10 μg/ml of NO-VN (*A*), or control VN (*B* and *C*) as 100%. The data were analyzed by Student's *t* test. *D*, the time dependence of rHSC spreading on 10 μg/ml VNs. Data are expressed by taking that of NO-VN at 120 min as 100%. Photomicrographs at 40× magnification of 10 μg/ml VNs are shown on the *right*, and the absolute values of total cells attached per view are shown in *parentheses* (*A–C*). The data represent the means ± S.D. ($n = 6$); ***, $p < 0.001$; **, $p < 0.01$; and *, $p < 0.05$ compared with that on NO- or control VN. The ratios of spreading cells/total cells (%) on 10 μg/ml NO- or control VN at 90 min (*A–C*) or 120 min (*D*), which were taken as 100% are: 59.7 ± 2.9 (*A*), 62.7 ± 5.9 (*B*), 70.5 ± 3.5 (*C*), and 89.8 ± 7.3 (*D*).

Reduction and S-Carboxymethylation of VNs—Each VN (50 μg) was dissolved in 270 μl of 0.5 M Tris-HCl buffer (pH 8.5) containing 8 M guanidine hydrochloride. After the addition of 2 μl of 2-mercaptoethanol, the mixture was incubated at room temperature for 2 h. Then, 5.67 mg of sodium iodoacetate was added, and the resulting mixture was incubated at room temperature in the dark for 2 h (24). The reaction mixture was applied to a PD-10 column (Amersham Biosciences) to remove the reagents, eluted by 10 mM Tris-HCl (pH 8.0), and concentrated to 1 ml in a SpeedVac. Reduced and carboxymethylated VNs were incubated with 2.5 μg/μl endopeptidase Glu-C overnight at 37 °C. The digested samples were completely dried and used for site-specific glycosylation analysis.

Site-specific Glycosylation Analysis of Glu-C-digested VNs—Glu-C-digested VNs were analyzed by LC/ESI-MS^n. LC/ESI-MS^n was carried out using on a Paradigm MS^4 system equipped with a Magic C18 column (0.2 × 50 mm, Michrome BioResources, Auburn, CA) connected to an LTQ ion trap mass spectrometer (Thermo Fisher Scientific, Waltham, MA). The eluants consisted of water containing 2% (v/v) acetonitrile and 0.1% (v/v) formic acid (pump A) and 90% acetonitrile and 0.1% formic acid (pump B). Glu-C-digested samples of VNs were eluted with 5% B for 10 min, followed by a linear gradient from 5% to 65% of pump B in 40 min at a flow rate of 3 μl/min. Mass spectra were recorded with sequential scans: a full MS scan (m/z 300–2000) by ion trap mass spectrometry in positive ion mode, followed by data-dependent MS^2 and MS^3 for the most abundant ion, and a scan (m/z 300–2000) by ion trap mass spectrometry in negative ion mode, followed by data-dependent two-stage mass spectrometry (MS^2) and three-stage mass spectrometry (MS^3) for the most abundant ion. The ESI voltage was set at 1.8 kV, and the capillary temperature was 200 °C.

Pyridylamination of VN Glycans—VNs (50 μg) were reduced and *S*-carboxymethylated as described above. The *N*-linked oligosaccharides were released with PNGase F (8 units) (10) and fluoresceinated with 2-aminopyridine (= d0-AP) or hexadeuterium-labeled 2-aminopyridine (d6-AP) as described previously (25). The pyridylaminated (PA-) oligosaccharides were desalted using an ENVI-Carb C column (Supelco Co., Ltd., Bellefonte, PA) and subjected to LC/MS^n.

Analysis of PA-oligosaccharides by Mass Spectrometry—PA-oligosaccharides of VNs were analyzed by LC/MS^n. LC/MS was performed using a Fourier transform ion cyclotron resonance/

ion trap mass spectrometer (LTQ-FT, Thermo Fisher Scientific) connected to a Magic 2002 high-performance liquid chromatography system (Michrom BioResource). The eluants were 5 mM CH_3COONH_4 (pH 9.6)-2% CH_3CN (pump A) and 5 mM CH_3COONH_4 (pH 9.6)-80% CH_3CN (pump B). The PA-*N*-linked oligosaccharides were separated on a Hypercarb column (0.2 × 150 mm, Thermo Fisher Scientific) with a 10–45% linear gradient of eluant B in 60 min at a flow rate of 2 μl/min. Mass spectra were recorded with sequential scans: a full MS scan (*m*/*z* 800–2000) by Fourier transform ion cyclotron resonance/ion trap mass spectrometry in positive ion mode, followed by data-dependent MS^2, MS^3, and MS^4 scans for the most abundant ion. The ESI voltage was set at 2.0 kV, a capillary temperature of 275 °C, resolution of Fourier transform ion cyclotron resonance/ion trap mass spectrometry of 50,000, and collision energy of 25% for MS^n experiments.

Two-dimensional Gel Electrophoresis—A pH 4–7 ReadyStrip IPG Strip (18 cm, Bio-Rad) was soaked in 5 ml of pH-gradient isoelectric focusing lysis buffer containing 1.8 g of urea, 100 μl of Pharmalyte 3–10 (Amersham Biosciences), 2.5 mM acetic acid, and 0.0025% orange G (Sigma). VNs (5 μg dialyzed against 10 mM Tris-HCl (pH 7.5)) were applied to the strip and isoelectrically focused using a CoolPhoreStar pH-gradient isoelectric focusing device (Anatech, Tokyo, Japan). The voltage was 500 V for the initial 120 min, 700 V for the following 60 min, followed by gradually increasing voltage for 60 min each at 1000, 1500, 2000, 2500, 3000, and finally 3500 V overnight at 20 °C. After the pH-gradient isoelectric focusing, the strip was equilibrated with 5 ml of SDS-equilibration buffer containing 0.9 g of urea, 0.01 M Tris (pH 6.8), 1% (v/v) SDS, 30% (v/v) glycerol, and 0.0125% bromphenol blue for 30 min. Two-dimensional separation was carried out by SDS-PAGE using 7.5% polyacrylamide gels (18 × 18 cm). SDS-PAGE gels were transferred to a polyvinylidene difluoride membrane and immunostained using sheep anti-VN IgGs (Binding Site Ltd.) or S2–566, an anti-oligosialic acid monoclonal antibody, and HRP-conjugated secondary antibodies. Membranes were developed with ECL-Plus (Amersham Biosciences).

RESULTS

Effects of Glycosylation of VNs on Cell Spreading—VN induces cell spreading through αvβ3 and αvβ5 integrins (26). Previously, we found a reduction of molecular mass of PH-VN due to a decrease in the carbohydrate concentration (15). In this study, NO-, SH-, and PH-VNs were purified from each plasma, and the effects of the changes in VN glycosylation on the cell spreading were observed by using rHSCs. The effect of PH-VN on rHSC spreading was found to be decreased to one-half of that of NO- or SH-VN (Fig. 1*A*). rHSC spreading was also decreased on neuraminidase-treated VN compared with untreated VN (Fig. 1*B*), whereas it was decreased less on de-*N*-glycosylated NO-VN (Fig. 1*C*). The time dependence analysis showed a gradual decrease in the rate of cell spreading on PH-VN, whereas that on neuraminidase-treated VN was significant with a shorter incubation (Fig. 1*D*). These results indicate the importance of glycosylation, particularly sialylation, of VN in rHSC spreading. The effect of de-*N*-glycosylation was small compared with that of desialylation (Fig. 1*B*), because many

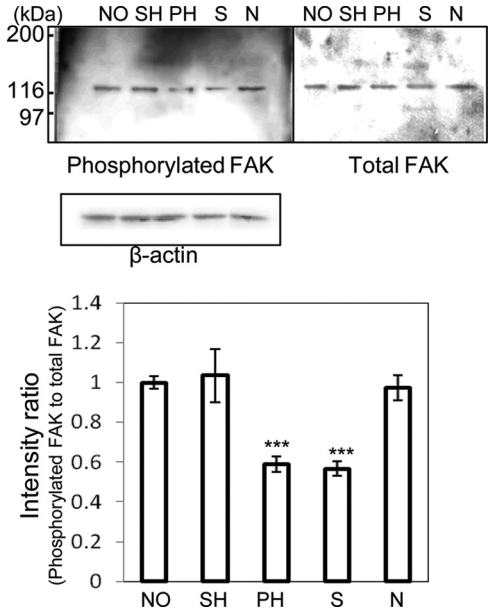

FIGURE 2. **Amounts of phosphorylated and total FAK in rHSCs.** rHSCs were detached and replated on dishes coated with NO-, SH-, PH-, desialylated, or de-*N*-glycosylated VN (10 μg/ml) for 90 min. The cell lysates were immunoblotted with anti-phosphotyrosine antibody (PY-20) to detect phosphorylated FAK as described in the text. Immunostaining of phosphorylated FAK, total FAK, and β-actin is shown in the *upper panels*. The relative amount of phosphorylated FAK, normalized to total FAK, was calculated by using the software program Scion Image and expressed by taking the intensity of the band of NO-VN as 1. The data represent the means ± S.D. ($n = 3$, meaning three separate experiments) and were analyzed by Student's *t* test; ***, $p < 0.001$ compared with NO-VN. Abbreviations: *S*, desialylated VN; *N*, de-*N*-glycosylated VN.

sialic acid residues still remained on the *O*-glycans after PNGase F-treatment. In addition, PNGase F converts asparagine to aspartate, which may reduce the effect of the decrease of the negative charge of sialic acids. Because a clear difference between de-*N*-glycosylated and non-treated samples in cell spreading was still observed (Fig. 1*C*), suggesting the contribution of *N*-glycans to some extent, it cannot be concluded from this result that *O*-glycans contribute more to the decreased rHSC spreading activity of PH-VN than *N*-glycans do.

Tyrosine Phosphorylation of FAK—To address the effects of glycosylation of VN on integrin-mediated signaling, FAK of rHSCs was compared among NO-, SH-, and PH-VN. As shown in Fig. 2, the amount of phosphorylated FAK on PH-VN was decreased proportional to cell spreading. These results suggest that the change in the glycosylation of VN due to partial hepatectomy is able to regulate activation of the integrin-mediated signaling pathway. In addition, the phosphorylated FAK on neuraminidase-treated NO-VN was decreased to a similar extent to that on PH-VN, whereas the total amounts of FAK were almost unchanged among all the VNs tested. Combined, the results indicate that the increased multimerization of VN decreased the FAK phosphorylation in rHSCs.

Site-specific Glycosylations of Rat VN—NO-, SH-, and PH-VNs were *S*-carboxymethylated, followed by digestion with Glu-C. The digested samples of VNs were analyzed by LC/ESI-MS^n. Identification of the peptide moieties of glycopeptides was based on the *m*/*z* values of peptide-related ions observed by MS^2 and MS^3, as described previously (27). Fig. 3 shows an MS^2

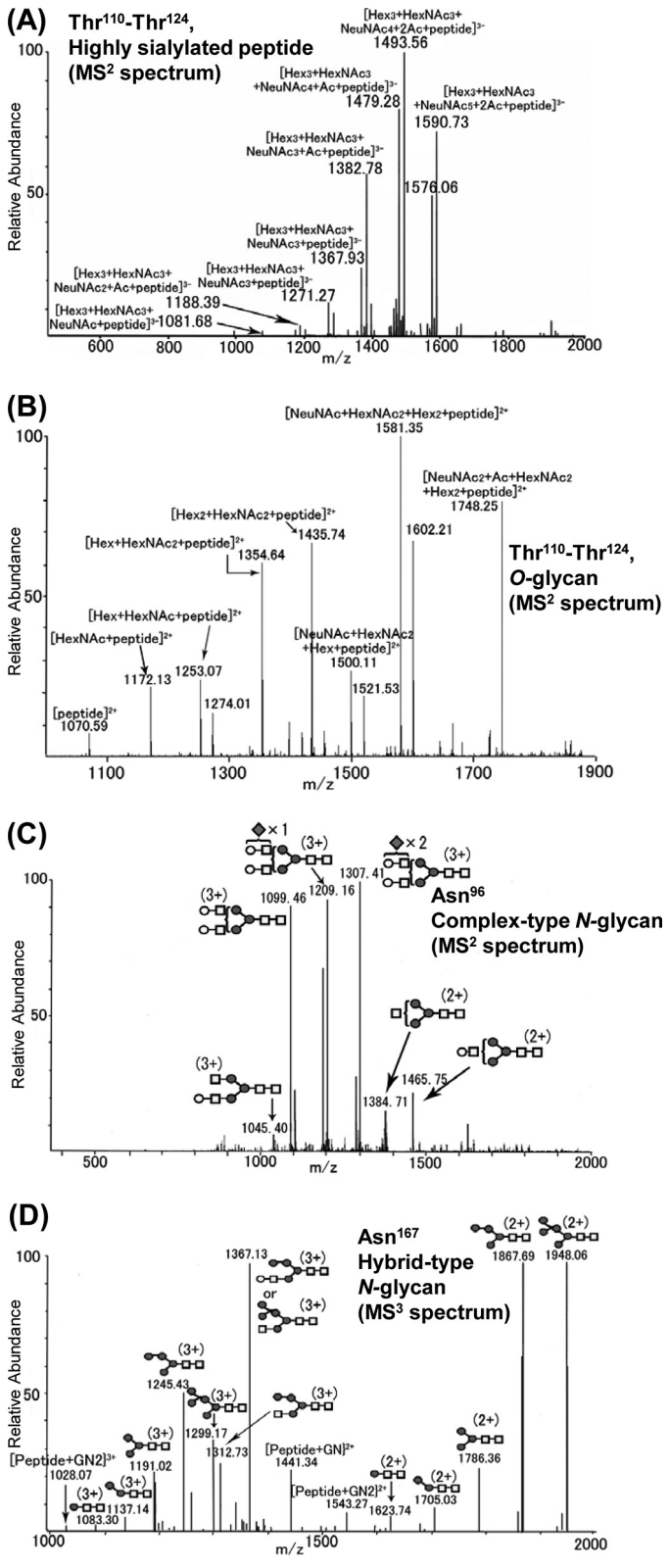

FIGURE 3. **Site-specific glycosylation analyses of rat VNs.** Mass spectra of *O*- and *N*-glycosylated peptides containing Ser/Thr$^{110-124}$ (*A* and *B*), Asn^{96} (*C*), and Asn^{167} (*D*). *A*, MS^2 of *m/z* 1687.72 (precursor ion, [Hex3HexNAc3NeuNAc6 + 2Ac + peptide − 3H]$^{3-}$) in negative ion mode, and *B*, MS^2 of *m/z* 1893.76 in positive ion mode ([NeuNAc3 + Ac + HexNAc2 + Hex2 + peptide − 2H]$^{2+}$, highly sialylated *O*-glycan) at 27 min (retention time of high-performance liquid chromatography). *C*, MS^2 of the product ion scan of *m/z* 1404.90 (MS^2) from MS ([Hex5HexNAc4NeuNAc3 + peptide − 3H]$^{3+}$, biantennary complex-type *N*-glycan with three NeuNAc units) at 30 min. *D*, MS^3 of the fragment ion at *m/z* 1421.19 ([Hex6HexNAc3 + peptide − 3H]$^{3+}$, MS^2) from MS of *m/z* 1629.36 ([Hex6HexNAc3NeuNAc2 + Ac + peptide − 3H]$^{3+}$, biantennary hybrid-type *N*-glycan) at 41 min. Abbreviations: *Ac*, *O*-acetyl residue; *Hex*, hexose; *HexNAc*, *N*-acetylhexosamine. *Symbols*: *diamond*, sialic acid; *open circle*, galactose; *square*, *N*-acetylglucosamine; *closed circle*, mannose; *triangle*, fucose.

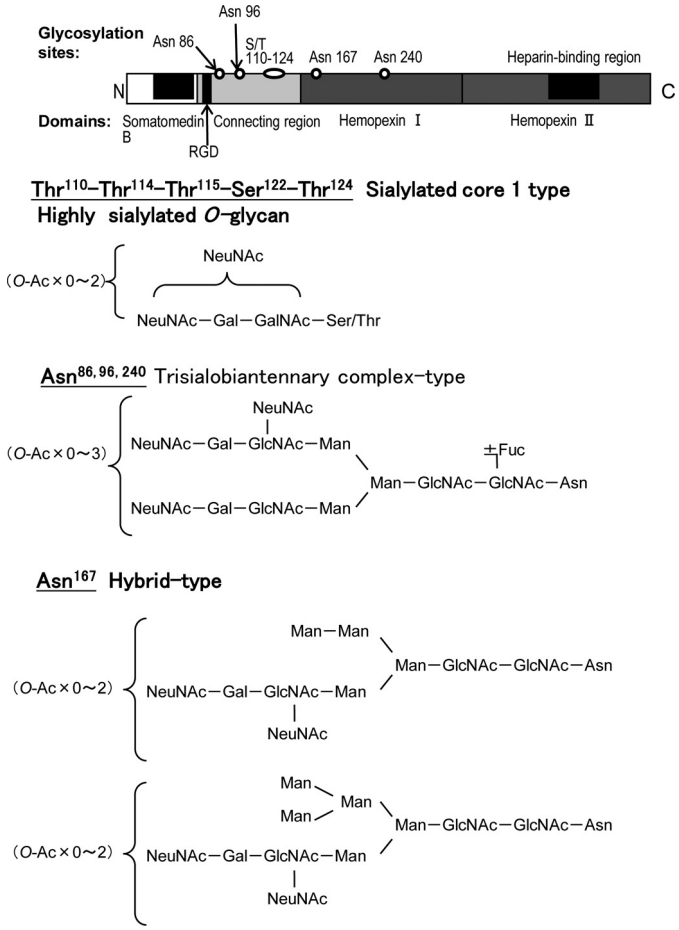

FIGURE 4. **Site-specific glycosylation of rat plasma VN.** The four glycosylation sites on rat plasma VN and the glycan structures at each glycosylation site were determined by glycopeptide analyses using LC/MS^n. The most frequent glycan structures that were present at each site are presented.

spectrum of a Thr^{110}–Glu^{128} peptide combined with sialylated *O*-glycans (*m/z* 1687.7) (Fig. 3, *A* and *B*), MS^2 spectrum of the Asn^{96}–Glu^{108} glycopeptide attached to a biantennary complex-type *N*-glycan with three NeuNAc units (*m/z* 1404.9) (Fig. 3*C*), and an MS^3 spectrum of the fragment ion (*m/z* 1421.19) observed by MS^2 of the Leu^{153}–Asn^{167}–Glu^{176} glycopeptide attached to a biantennary hybrid-type *N*-glycan (*m/z* 1629.4) (Fig. 3*D*). The peptides of residues Thr^{110}–Thr^{124} were *O*-glycosylated, whereas four potential sites, Asn^{86}, Asn^{96}, Asn^{167}, and Asn^{240} were revealed to be *N*-glycosylated. In the Thr^{110}–Thr^{124} region, the highly sialylated glycans were detected in the negative ion mode spectrum (Fig. 3*A*), and the analysis in positive ion mode revealed that a Hex-HexNAc unit was located in the inner region of the glycans (Fig. 3*B*). From the results of lectin reactivity (15), it was inferred that one to three sialylated core-1 type molecules was attached. The mass spectra acquired from NO-VN and PH-VN suggested a decrease in the *O*-glycosylation on the peptide due to partial hepatectomy

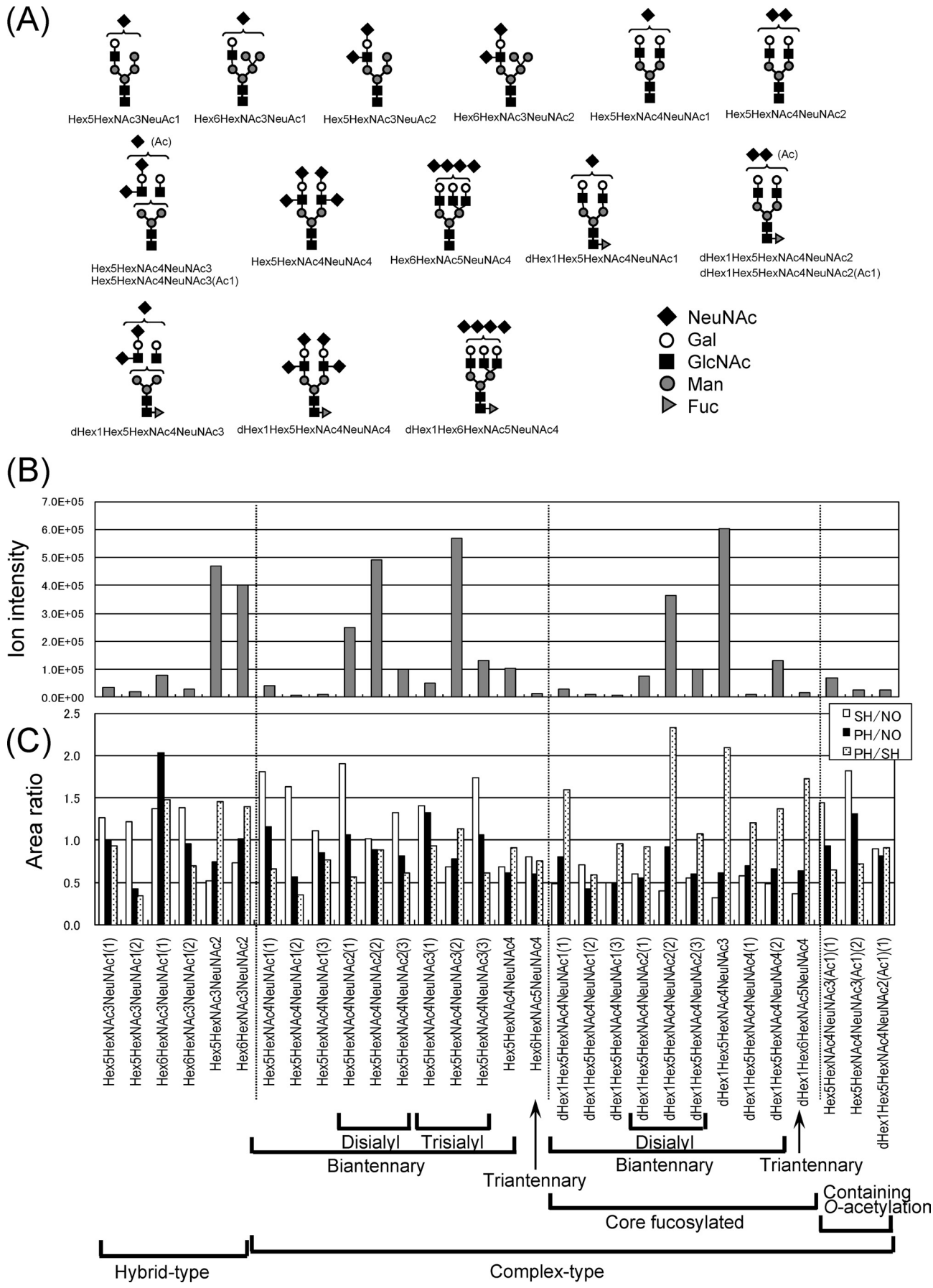
(A)
Hex5HexNAc3NeuAc1
Hex6HexNAc3NeuAc1
Hex5HexNAc3NeuAc2
Hex6HexNAc3NeuNAc2
Hex5HexNAc4NeuNAc1
Hex5HexNAc4NeuNAc2
(Ac)
Hex5HexNAc4NeuNAc3
Hex5HexNAc4NeuNAc3(Ac1)
Hex5HexNAc4NeuNAc4
Hex6HexNAc5NeuNAc4
dHex1Hex5HexNAc4NeuNAc1
(Ac)
dHex1Hex5HexNAc4NeuNAc2
dHex1Hex5HexNAc4NeuNAc2(Ac1)
dHex1Hex5HexNAc4NeuNAc3
dHex1Hex5HexNAc4NeuNAc4
dHex1Hex6HexNAc5NeuNAc4
NeuNAc
Gal
GlcNAc
Man
Fuc
(B)
Ion intensity
7.0E+05
6.0E+05
5.0E+05
4.0E+05
3.0E+05
2.0E+05
1.0E+05
0.0E+00
(C)
Area ratio
2.5
2.0
1.5
1.0
0.5
0.0
SH/NO
PH/NO
PH/SH
Hex5HexNAc3NeuNAc1(1)
Hex5HexNAc3NeuNAc1(2)
Hex6HexNAc3NeuNAc1(1)
Hex6HexNAc3NeuNAc1(2)
Hex5HexNAc3NeuNAc2
Hex6HexNAc3NeuNAc2
Hex5HexNAc4NeuNAc1(1)
Hex5HexNAc4NeuNAc1(2)
Hex5HexNAc4NeuNAc1(3)
Hex5HexNAc4NeuNAc2(1)
Hex5HexNAc4NeuNAc2(2)
Hex5HexNAc4NeuNAc2(3)
Hex5HexNAc4NeuNAc3(1)
Hex5HexNAc4NeuNAc3(2)
Hex5HexNAc4NeuNAc3(3)
Hex5HexNAc4NeuNAc4
Hex6HexNAc5NeuNAc4
dHex1Hex5HexNAc4NeuNAc1(1)
dHex1Hex5HexNAc4NeuNAc1(2)
dHex1Hex5HexNAc4NeuNAc1(3)
dHex1Hex5HexNAc4NeuNAc2(1)
dHex1Hex5HexNAc4NeuNAc2(2)
dHex1Hex5HexNAc4NeuNAc2(3)
dHex1Hex5HexNAc4NeuNAc3
dHex1Hex5HexNAc4NeuNAc4(1)
dHex1Hex5HexNAc4NeuNAc4(2)
dHex1Hex6HexNAc5NeuNAc4
Hex5HexNAc4NeuNAc3(Ac1)(1)
Hex5HexNAc4NeuNAc3(Ac1)(2)
dHex1Hex5HexNAc4NeuNAc2(Ac1)(1)
Disialyl
Trisialyl
Biantennary
Triantennary
Disialyl
Biantennary
Triantennary
Containing
O-acetylation
Core fucosylated
Hybrid-type
Complex-type

(see supplemental Fig. 1). The most frequent *N*-glycan structures site-specifically found for each site are shown in Fig. 4. At Asn^{86}, Asn^{96}, and Asn^{240}, biantennary complex-type trisialoglycans with or without core fucosylation and with different amounts of *O*-acetylated NeuNAc were deduced (Fig. 4), whereas biantennary hybrid-type *N*-glycans were found to be the major structures at Asn^{167}. The MS^3 of the fragment ion at *m*/*z* 1421.19 (MS^2) from MS of *m*/*z* 1629.36 at 41 min is shown in Fig. 3*D*.

Quantitative Analysis of N-Linked Glycans of Rat VNs—Pyridylaminated (PA) *N*-glycans from NO-, SH-, and PH-VNs were analyzed by LC/MS^n for relative quantification. The predicted *N*-glycan structures of NO-VN and each ionic intensity are shown in Fig. 5 (*A* and *B*). Besides the major biantennary complex-type structure, triantennary complex and hybrid structures were detected. No significant change in the structural variation of the *N*-glycans was found among NO-, SH-, and PH-VNs (data not shown).

The *N*-glycans released from equal amounts of each VN were tagged with d0- or d6-AP, and the PA-oligosaccharides from both kinds of the three VNs were co-injected into LC/MS as described previously (25) to estimate the change in the amount of each *N*-glycan structure. The ionic intensities of each glycan were compared and are shown in Fig. 5*C*. In the hybrid-type *N*-glycans, Hex6HexNAc3NeuNAc1, Hex5HexNAc3NeuNAc2, and Hex6HexNAc3NeuNAc2 (Hex: hexose, HexNAc: *N*-acetylhexosamine, NeuNAc: *N*-acetylneuraminic acid, the number of each monosaccharide in the glycan is shown following the abbreviation) increased in PH-VN compared with SH-VN, as shown on the *left side* of Fig. 5*C*. The fucosylation ratios were remarkably increased, whereas glycosylation was decreased in all PH-VN compared with that of NO-VN, as shown in the center of Fig. 5*C*, in accordance with the results of examinations of carbohydrate compositions and reactivity with lectins described previously (15). Rat VN contained trisialobiantennary complex glycans with or without core fucosylation as the most common *N*-glycans, and disialobiantennary complex and hybrid glycans were also included as major components; on the last point, VN is different from rat plasma fibronectin (18).

Change in Isoelectric Points and Oligosialylation of VN—We previously showed that rat plasma VN has a diNeuAc structure that is remarkably decreased 24 h after partial hepatectomy according to chemical analysis and immunoreactivity (22). Highly sialylated *O*-glycans (Figs. 3*D* and 4), which were markedly decreased in PH-VN, are likely to have a diNeuAc structure that affects the isoelectric points of VNs. Immunostaining of VNs after two-dimensional PAGE showed that each VN has two components, pI 4.0 and 5.7 in NO-VN, that both shifted to higher pI, pI 4.3 and 6.0 in SH-VN, and further to pI 4.6 and 6.0 in PH-VN (Fig. 6, *A*–*C*). The pI of NO-VN was converted to one basic point, pI 6, after neuraminidase treatment (Fig. 6*D*), and only the more acidic component of pI 4.1 reacted with mAb S2–566, which specifically recognizes the Neu5Acα2,8Neu5Acα2,3Gal structure (22) (Fig. 6*E*). Comparing PH-VN to SH-VN, the shift to a higher pI of the acidic component was more remarkable than that of the more basic component. These results clearly indicate that sialylation decreased the most in PH-VN and to a lesser extent in SH-VN and that the decrease of oligosialylation was particularly remarkable in PH-VN.

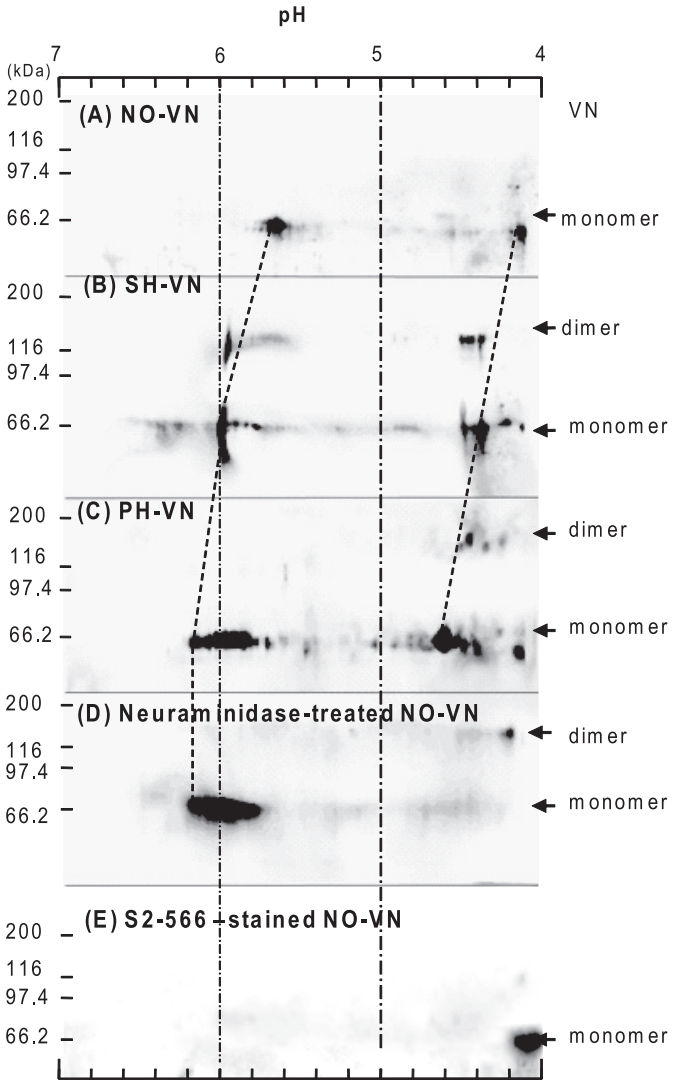

FIGURE 6. **Two-dimensional PAGE and Western blotting of VNs.** The first electrophoresis was isoelectric focusing. The second electrophoresis was SDS-PAGE under reducing conditions on 7.5% polyacrylamide gel, followed by blotting onto a polyvinylidene difluoride membrane and immunostaining using sheep anti-VN IgGs (*A*–*D*) or the anti-oligosialic acid monoclonal antibody S2–566 (*E*), and HRP-conjugated secondary antibodies as described in the text. Membranes were developed with ECL-Plus.

DISCUSSION

This study showed for the first time that adhesion and spreading of rHSC and FAK phosphorylation were concomitantly suppressed on PH-VN (Fig. 1), indicating that integrin

FIGURE 5. **Structures and intensities of *N*-glycans of rat VN.** The *N*-glycans of rat VN were reacted with a fluorescent probe, 2-aminopyridine, and analyzed by LC/MS^n. *A*, the *N*-glycan structures of VN. *Symbols*: *diamond*, sialic acid; *open circle*, galactose; *square*, *N*-acetylglucosamine; *closed circle*, mannose; *triangle*, fucose. *B*, ionic intensity of each *N*-glycan of NO-VN ($n = 3$). *C*, the ionic intensities of each glycan of the PH-, SH-, and NO-VNs were compared. Relative ratios of each glycan are expressed by taking that of NO-VN as 1 ($n = 2$). *Open bar*, SH/NO; *solid bar*, PH/NO; *dotted bar*, PH/SH.

signaling was attenuated through interaction with PH-VN. Enzymatic desialylation of VN decreased the rHSC-spreading activity (Fig. 1*B*), suggesting that the decrease in PH-VN activity was caused by decreased sialylation (Figs. 1 and 2). At 24 h after operation, most PH-VN is considered to have been synthesized in the early stage of liver regeneration after partial hepatectomy, because the half-life of VN in the blood circulation is about 8 h (28). In support, the structures and changes of rat VN glycans during liver regeneration after partial hepatectomy were elucidated. Rat VN has a site-specific hybrid-type *N*-glycans at Asn^{167} and a highly sialylated *O*-glycan in the Thr^{110}–Thr^{124} region. In PH-VN, the ratios of fucosylation of *N*-glycans and hybrid-type glycans were increased compared with SH-VN (Fig. 5), whereas sialylation was remarkably decreased (Fig. 6).

As described above, the changes in glycosylation of postoperative VNs can modulate the survival, activation, and proliferation of HSCs during liver regeneration, because substrate adhesion and spreading are prerequisites for activation and proliferation of HSCs. HSCs are the major source of the newly produced ECM that accumulates in fibrotic liver. Activation of HSCs is therefore responsible for the development of liver fibrosis in chronic liver diseases of all causes, whereas extensive HSC apoptosis coincident with the degradation of ECM occurs during the resolution of fibrosis (19). Therefore, the clearance of unbound HSCs by apoptosis may allow the recovery from liver injury and reversal of liver fibrosis. The fate of stellate cells was reported to be influenced by ECM through $\alpha v\beta 3$ integrin (26), which is a major receptor for VN, followed by activation of FAK, which binds to Src family kinases and other intracellular signaling molecules, to trigger multiple downstream pathways to regulate cell survival (29). Our findings suggest that the removal of sialic acid from VN suppresses the activation of stellate cells, indicating the possibility of a new treatment or method of prevention for liver cirrhosis.

The mRNA level of VN was reported not to change after partial hepatectomy and sham operation (30). We found that plasma VN obtained from PH rats had low carbohydrate concentrations, suggesting that PH-VN was less glycosylated (15). The decreased *N*-glycosylation of VN at 24 h after partial hepatectomy could be attributed to the attenuation of the oligosaccharide transferase activity in microsomes (31, 32), which also causes the decrease of total glycoprotein synthesis in regenerating liver (33). In the early stage after partial hepatectomy, amounts of several kinds of fucosylated glycoprotein were reported to increase (34). Additionally, fucosyltransferase activity was reported to be increased during liver regeneration in hepatobiliary disease (35). In this study, core-fucosylated *N*-glycans in VN markedly increased after partial hepatectomy (Fig. 5). The observation of such changes of VN glycosylation after partial hepatectomy is consistent with the reported changes of related enzyme activities. On the one hand, we reported that rat VN is modified by disialic acid (22), the presence of diNeuAc structures was described in some glycoproteins more than three decades ago (36), and neural cell adhesion molecules have been very thoroughly studied (2). Changes in the expression of the oligosialic epitope on serum glycoproteins under inflammatory conditions were also reported (37, 38). The fact that diNeuAc in PH-VN was decreased compared with that in NO-VN indicates that the inflammation caused by partial hepatectomy reduces the amount of diNeuAc on VN, although inflammation caused by turpentine oil does not change the disialylation level in serum (22). In this study, we found that the sialylation of VN plays an important role in rHSC spreading (Fig. 1). The analysis of isoelectric points showed that the oligosialic acid on the *O*-glycan significantly affects the pI of acidic PH-VN fraction (Fig. 6). In addition to the decrease of oligosialyl epitopes in PH-VN, the undersialylation of both *N*- and *O*-glycans was found in the basic PH-VN fraction (Fig. 6). These results indicate that the decreased sialylation plays a key role in regulating the function of VN in liver regeneration.

As for the biological significance of the changes in glycosylation, including sialylation, we previously reported that the collagen-binding activity of VN increased coincident with the increase of the multimerization state (16). It is presumed that the decrease of intermolecular electrostatic repulsion of polyanions on oligosialic acid contributes to promotion of multimerization of VN. The oligosialic *O*-glycosylation site is localized in a region that has been suggested to undergo a conformational change to allow exposure accompanying the activation, followed by multimerization of VN (39). The enhanced collagen binding of VN may contribute to fibrogenesis and tissue degradation in combination with the concentration of tissue lytic factors that are associated with VN.

This study proposes that the alteration of glycosylation of PH-VN is very significant in the modulation of the adhesion of HSCs, which is a key step to matrix restructuring. In this context, understanding the modulation of glycans on VN may contribute to the development of a strategy to regulate matrix deposition in liver cirrhosis. Further studies will focus on the regulation of rHSC activation, proliferation, and apoptosis due to glycosylation of VN and elucidation of the molecular mechanisms of liver regeneration from the viewpoint of alterations in glycosylation of ECM.

Acknowledgments—We thank Dr. Mitsuru Sato of Akita University School of Medicine for providing rHSC, our laboratory members for helping with the operations, and K. Ono for editing the English.

REFERENCES

1. DeClerck, Y. A., Mercurio, A. M., Stack, M. S., Chapman, H. A., Zutter, M. M., Muschel, R. J., Raz, A., Matrisian, L. M., Sloane, B. F., Noel, A., Hendrix, M. J., Coussens, L., and Padarathsingh, M. (2004) *Am. J. Pathol.* **164,** 1131–1139
2. Varki, A. (1993) *Glycobiology* **3,** 97–130
3. Schvartz, I., Seger, D., and Shaltiel, S. (1999) *Int. J. Biochem. Cell Biol.* **31,** 539–544
4. Podack, E. R., Kolb, W. P., and Müller-Eberhard, H. J. (1977) *J. Immunol.* **119,** 2024–2029
5. McKeown-Longo, P. J., and Panetti, T. S. (1996) *Trends Glycosci. Glycotechnol.* **8,** 327–340
6. Seiffert, D., Keeton, M., Eguchi, Y., Sawdey, M., and Loskutoff, D. J. (1991) *Proc. Natl. Acad. Sci. U.S.A.* **88,** 9402–9406
7. Seiffert, D. (1997) *Histol. Histopathol.* **12,** 787–797
8. Preissner, K. T. (1991) *Annu. Rev. Cell Biol.* **7,** 275–310
9. Pretzlaff, R. K., Xue, V. W., and Rowin, M. E. (2000) *Cell Adhes. Commun.* **7,** 491–500
10. Yoneda, A., Kojima, K., Matsumoto, I., Yamamoto, K., and Ogawa, H.

(1996) *J. Biochem.* **120,** 954–960
11. Yoneda, A., Ogawa, H., Matsumoto, I., Ishizuka, I., Hase, S., and Seno, N. (1993) *Eur. J. Biochem.* **218,** 797–806
12. Ogawa, H., Yoneda, A., Seno, N., Hayashi, M., Ishizuka, I., Hase, S., and Matsumoto, I. (1995) *Eur. J. Biochem.* **230,** 994–1000
13. Kitagaki-Ogawa, H., Yatohgo, T., Izumi, M., Hayashi, M., Kashiwagi, H., Matsumoto, I., and Seno, N. (1990) *Biochim. Biophys. Acta* **1033,** 49–56
14. Yoneda, A., Ogawa, H., Kojima, K., and Matsumoto, I. (1998) *Biochemistry* **37,** 6351–6360
15. Uchibori-Iwaki, H., Yoneda, A., Oda-Tamai, S., Kato, S., Akamatsu, N., Otsuka, M., Murase, K., Kojima, K., Suzuki, R., Maeya, Y., Tanabe, M., and Ogawa, H. (2000) *Glycobiology* **10,** 865–874
16. Sano, K., Asanuma-Date, K., Arisaka, F., Hattori, S., and Ogawa, H. (2007) *Glycobiology* **17,** 784–794
17. Asanuma, K., Arisaka, F., and Ogawa, H. (2001) *International Congress Series* **1223,** 97–101
18. Sano, K., Asahi, M., Yanagibashi, M., Hashii, N., Itoh, S., Kawasaki, N., and Ogawa, H. (2008) *Carbohydr. Res.* **343,** 2329–2335
19. Benyon, R. C., and Arthur, M. J. (2001) *Semin. Liver Dis.* **21,** 373–384
20. Yatohgo, T., Izumi, M., Kashiwagi, H., and Hayashi, M. (1988) *Cell Struct. Funct.* **13,** 281–292
21. Ueda, H., Kojima, K., Saitoh, T., and Ogawa, H. (1999) *FEBS Lett.* **448,** 75–80
22. Yasukawa, Z., Sato, C., Sano, K., Ogawa, H., and Kitajima, K. (2006) *Glycobiology* **16,** 651–665
23. Higgins, G. M., and Anderson, R. M. (1931) *Arch. Pathol.* **12,** 186–202
24. Harazono, A., Kawasaki, N., Kawanishi, T., and Hayakawa, T. (2005) *Glycobiology* **15,** 447–462
25. Yuan, J., Hashii, N., Kawasaki, N., Itoh, S., Kawanishi, T., and Hayakawa, T. (2005) *J. Chromatogr. A.* **1067,** 145–152
26. Zhou, X., Murphy, F. R., Gehdu, N., Zhang, J., Iredale, J. P., and Benyon, R. C. (2004) *J. Biol. Chem.* **279,** 23996–24006
27. Itoh, S., Kawasaki, N., Harazono, A., Hashii, N., Matsuishi, Y., Kawanishi, T., and Hayakawa, T. (2005) *J. Chromatogr. A* **1094,** 105–117
28. Peake, P. W., Greenstein, J. D., Pussell, B. A., and Charlesworth, J. A. (1996) *Clin. Exp. Immunol.* **106,** 416–422
29. Zhao, J., and Guan, J. L. (2009) *Cancer Metastasis Rev.* **28,** 35–49
30. Kim, T. H., Mars, W. M., Stolz, D. B., Petersen, B. E., and Michalopoulos, G. K. (1997) *Hepatology* **26,** 896–904
31. Oda-Tamai, S., Kato, S., Hara, S., and Akamatsu, N. (1985) *J. Biol. Chem.* **260,** 57–63
32. Okamoto, Y., Ito, E., and Akamatsu, N. (1978) *Biochim. Biophys. Acta* **542,** 21–27
33. Okamoto, Y., and Akamatsu, N. (1977) *Biochim. Biophys. Acta* **498,** 272–281
34. Kato, S., and Akamatsu, N. (1985) *Biochem. J.* **229,** 521–528
35. Jezequel-Cuer, M., Dalix, A. M., Flejou, J. F., and Durand, G. (1992) *Liver* **12,** 140–146
36. Finne, J., Krusius, T., and Rauvala, H. (1977) *Biochem. Biophys. Res. Commun.* **74,** 405–410
37. Yasukawa, Z., Sato, C., and Kitajima, K. (2005) *Glycobiology* **15,** 827–837
38. Yasukawa, Z., Sato, C., and Kitajima, K. (2007) *J. Biochem.* **141,** 429–441
39. Stockmann, A., Hess, S., Declerck, P., Timpl, R., and Preissner, K. T. (1993) *J. Biol. Chem.* **268,** 22874–22882